A NOTE ON THE APPROXIMATION PROPERTIES OF THE LOCALLY DIVERGENCE-FREE FINITE ELEMENTS

JIANGGUO LIU AND RACHEL CALI

(Communicated by Peter Minev)

Abstract. This paper investigates construction and approximation properties of the locally divergence-free (LDF) finite elements. Numerical stability of the natural and normalized bases for the LDF elements is analyzed. Error estimates about the jumps and the total divergence of the localized $\mathbf{L}_2$-projection are proved and validated through numerical examples.

Key Words. approximation property, locally divergence-free (LDF), localized $\mathbf{L}_2$-projection, solenoidal

1. Introduction

"Divergence-free" is an important physical property that appears in many applications, for example, incompressible fluid flows and solenoidal magnetic fields. The divergence-free property should be preserved by numerical methods, globally or locally, in the classical or weak sense [7]. An early study on magnetohydrodynamics (MHD) [4] has shown that numerical errors in the divergence of a magnetic field may build up in time and bring up nonphysical phenomena in numerical simulations, for instance, loss of momentum and energy conservation.

The locally divergence-free finite elements [1] have regained researchers' interests in recent years. The LDF elements are devised to preserve the divergence-free property locally or pointwise inside each element. These elements typically have polynomial shape functions. When the LDF elements are glued together to form an approximation subspace, continuity across element interfaces is usually lost. Continuity can be enforced in the normal directions of element interfaces to construct nonconforming LDF finite element approximation subspace. This approach is adopted in [5] for solving the reduced time-harmonic Maxwell equations. Another approach is to place the LDF finite elements in the framework of the discontinuous Galerkin methods and weak discontinuity is then enforced by penalty factors. Applications along this line can be found in [1, 10, 11] for solving stationary Stokes and Navier-Stokes problems, [8] for solving the Maxwell equations, and [13] for solving the ideal MHD problem.

For implementations of the LDF finite elements, the natural basis functions [1] are conceptually simple and appealing, but their divergence-free property is not preserved by affine mappings. In this paper, we will show that the natural basis functions are actually numerically unstable, so normalization on shape functions should be adopted. When the LDF elements are used in the discontinuous Galerkin framework, there are jumps across the element interfaces. In other words,

the "total divergence" of a numerical solution might not be zero. The jumps or the total divergence in LDF finite element approximations need to be measured. Especially, when the LDF elements are used with the characteristic methods [14], the foot/head of a characteristic might fall right on the interface of two elements. The localized $\mathbf{L}_2$-projection [3] could be used to approximate the initial solenoidal vector fields for time-dependent problems. How good could the localized $\mathbf{L}_2$-projection be (regarding the jumps or the total divergence)? This paper addresses the above issues. In Section 2, we show that the natural bases for the LDF elements are numerically unstable and propose some normalized bases for the LDF elements. Section 3 discusses the approximation properties of the LDF elements with a focus on the localized $\mathbf{L}_2$-projection. The theoretical error estimates are illustrated and validated in Section 4 through a very smooth vector field and a nonsmooth field.

Throughout the paper, we shall use $A \lesssim B$ to represent an inequality $A \leq CB$, where C is a generic positive constant independent of the mesh size.

2. Natural and Normalized Bases for the LDF Elements

"Locally divergence-free" is actually a pointwise property, unrelated to the geometric shapes of finite elements. It can be proved that for a two-dimensional vector field $\mathbf{v}$, it is divergence-free (div $\mathbf{v} = 0$) if and only if there exists a scalar potential function $A(x, y)$ such that

$$\mathbf{v}(x, y) = \mathbf{curl}\, A = \left(\frac{\partial A}{\partial y}, -\frac{\partial A}{\partial x} \right).$$

Therefore, one can take the curl of the natural basis polynomials

$$1,\ x,\ y,\ x^2,\ xy,\ y^2,\ x^3,\ x^2y,\ xy^2,\ y^3,\ \ldots$$

to get a natural basis for the LDF finite elements. Clearly, there are 2 zeroth-order and 3 first-order basis functions:

$$(1) \qquad \begin{pmatrix} 1 \\ 0 \end{pmatrix}, \begin{pmatrix} 0 \\ 1 \end{pmatrix}, \begin{pmatrix} y \\ 0 \end{pmatrix}, \begin{pmatrix} 0 \\ x \end{pmatrix}, \begin{pmatrix} x \\ -y \end{pmatrix}.$$

There are 4 second-order and 5 third-order basis functions:

$$(2) \qquad \begin{pmatrix} y^2 \\ 0 \end{pmatrix}, \begin{pmatrix} 0 \\ x^2 \end{pmatrix}, \begin{pmatrix} x^2 \\ -2xy \end{pmatrix}, \begin{pmatrix} -2xy \\ y^2 \end{pmatrix},$$

$$(3) \qquad \begin{pmatrix} y^3 \\ 0 \end{pmatrix}, \begin{pmatrix} 0 \\ x^3 \end{pmatrix}, \begin{pmatrix} x^3 \\ -3x^2y \end{pmatrix}, \begin{pmatrix} -3xy^2 \\ y^3 \end{pmatrix}, \begin{pmatrix} x^2y \\ -xy^2 \end{pmatrix}.$$

Three-dimensional natural bases for the LDF finite elements can be constructed similarly [1].

Although theoretically these basis functions can be used for any elements, they are numerically unstable. The mass/Gram matrix of these basis functions could be very ill-conditioned. For example, suppose we have a uniform rectangular mesh on the unit square $[0, 1] \times [0, 1]$ with a mesh size 0.01 in each direction. If we use all these natural basis functions up to order 3 on the rectangle element $[0, 0.01] \times [0, 0.01]$, then the condition number of the mass matrix measured in 2-norm is as high as 2.800×10^{15}. This could result in unpredictable round-off errors that fail the Cholesky factorization process in the localized $\mathbf{L}_2$-projection, to be discussed later in Section 3.

Therefore, some sort of local basis functions are needed for different elements. However, we may not use the affine mappings from generic elements to the reference

rectangle/triangle element that are commonly used in most finite element methods, since the divergence-free property will be lost by the affine mappings [11].

A remedy could be the following normalization transform

$$(4) \qquad X = \frac{x - x_c}{\sqrt{A}}, \quad Y = \frac{y - y_c}{\sqrt{A}},$$

where (x_c, y_c) is the center of the rectangle/triangle element and A is its area. We then obtain a new set of basis functions in almost identical forms, with the variables x, y in formulas (1,2,3) being replaced by X, Y:

$$(5) \qquad \begin{pmatrix} 1 \\ 0 \end{pmatrix}, \begin{pmatrix} 0 \\ 1 \end{pmatrix}, \begin{pmatrix} Y \\ 0 \end{pmatrix}, \begin{pmatrix} 0 \\ X \end{pmatrix}, \begin{pmatrix} X \\ -Y \end{pmatrix},$$

$$(6) \qquad \begin{pmatrix} Y^2 \\ 0 \end{pmatrix}, \begin{pmatrix} 0 \\ -X^2 \end{pmatrix}, \begin{pmatrix} X^2 \\ -2XY \end{pmatrix}, \begin{pmatrix} -2XY \\ Y^2 \end{pmatrix},$$

$$(7) \qquad \begin{pmatrix} Y^3 \\ 0 \end{pmatrix}, \begin{pmatrix} 0 \\ X^3 \end{pmatrix}, \begin{pmatrix} X^3 \\ -3X^2Y \end{pmatrix}, \begin{pmatrix} -3XY^2 \\ Y^3 \end{pmatrix}, \begin{pmatrix} X^2Y \\ -XY^2 \end{pmatrix}.$$

These normalized basis functions are still divergence-free, since they are linear combinations of the natural basis functions. For example,

$$\begin{pmatrix} X \\ -Y \end{pmatrix} = \frac{1}{\sqrt{A}} \begin{pmatrix} x \\ -y \end{pmatrix} - \frac{x_c}{\sqrt{A}} \begin{pmatrix} 1 \\ 0 \end{pmatrix} + \frac{y_c}{\sqrt{A}} \begin{pmatrix} 0 \\ 1 \end{pmatrix}.$$

But these normalized basis functions enjoy better numerical stability than the natural basis functions do. For example, the condition number of the mass matrix for the normalized basis functions up to order 3 on the rectangle element $[0, 0.01]^2$ is now reduced to 2.904×10^3.

The normalization transform (4) is good for triangle, rectangular, quadrilateral, or any other type of elements, and can be easily extended to three-dimensional LDF elements. It is also very convenient for implementation in object-oriented programming language. A C++ implementation for the two-dimensional LDF elements on unstructured meshes has been provided by the authors.

A set of $\mathbf{L}_2$-orthogonal basis functions up to order 3 are constructed in [8] for a generic rectangular element with center (x_c, y_c) and width $\Delta x, \Delta y$:

$$\begin{pmatrix} 1 \\ 0 \end{pmatrix}, \begin{pmatrix} 0 \\ 1 \end{pmatrix}, \begin{pmatrix} Y \\ 0 \end{pmatrix}, \begin{pmatrix} 0 \\ X \end{pmatrix}, \begin{pmatrix} \Delta x X \\ -\Delta y Y \end{pmatrix},$$

$$\begin{pmatrix} 12Y^2 - 1 \\ 0 \end{pmatrix}, \begin{pmatrix} 0 \\ 12X^2 - 1 \end{pmatrix}, \begin{pmatrix} \Delta x(12X^2 - 1) \\ -24\Delta y XY \end{pmatrix}, \begin{pmatrix} -24\Delta x XY \\ \Delta y(12Y^2 - 1) \end{pmatrix},$$

$$\begin{pmatrix} Y(20Y^2 - 3) \\ 0 \end{pmatrix}, \begin{pmatrix} 0 \\ X(20X^2 - 3) \end{pmatrix},$$

$$\begin{pmatrix} -\Delta x X(12Y^2 - 1) \\ \Delta y Y(4Y^2 - 1) \end{pmatrix}, \begin{pmatrix} \Delta x X(4X^2 - 1) \\ -\Delta y Y(12X^2 - 1) \end{pmatrix}, \begin{pmatrix} \Delta x Y(12X^2 - 1) \\ -\Delta y X(12Y^2 - 1) \end{pmatrix},$$

where

$$X = \frac{x - x_c}{\Delta x}, \quad Y = \frac{y - y_c}{\Delta y}.$$

However, these basis functions are good only for rectangle elements and the 5th, 8th, 9th, 12th, 13th, 14th functions in the above basis still exhibit *scale disparity*, due to the small values of $\Delta x, \Delta y$.

3. Approximation Properties of the LDF Finite Elements

Let $d = 2$ or 3 be the space dimension, $\Omega \subset \mathbb{R}^d$ be a domain with a Lipschitz boundary, and $D \subseteq \Omega$ a subdomain. For a nonnegative integer m, $H^m(D)$ denotes the usual Sobolev space with the inner product

$$(u, v)_{m,D} = \sum_{|\alpha| \leq m} \int_D \partial^\alpha u \, \partial^\alpha v \, d\mathbf{x}, \quad u, v \in H^m(D),$$

and the semi-norm

$$|u| = \left(\sum_{|\alpha|=m} \int_D |\partial^\alpha u|^2 \right)^{1/2},$$

where $\alpha = (\alpha_1, \ldots, \alpha_d)$ is a d-index. Then we define the Sobolev space of vector fields

$$\mathbf{H}^m(D) = (H^m(D))^d \quad \text{with} \quad (\mathbf{u}, \mathbf{v}) = \sum_{i=1}^d (u_i, v_i)_{m,D}$$

and the Sobolev space of solenoidal vector fields

$$\mathbf{S}^m(D) = \{\mathbf{v} \in \mathbf{H}^m(D) : \nabla \cdot \mathbf{v} = 0 \text{ on } D\}.$$

For a nonnegative integer $k \geq 0$, $P^k(D)$ denotes the space of polynomials of degree at most k on D and $\mathbf{P}^k(D) = (P^k(D))^d$. We then define

$$\mathbf{Q}^m(D) = \{\mathbf{q} \in \mathbf{P}^m(D) : \nabla \cdot \mathbf{q} = 0 \text{ on } D\}.$$

The following approximation properties are very useful.

Theorem 1 (Optimal approximation property)   *Let $m \geq 0$ be an integer and $D \subset \mathbb{R}^d$ a domain.*

 (i) *If $\mathbf{u} \in \mathbf{H}^{m+1}(D)$, then there exists $\mathbf{p} \in \mathbf{P}^m(D)$ such that for any integer $0 \leq k \leq m+1$,*

$$(8) \qquad \|\mathbf{u} - \mathbf{p}\|_{\mathbf{H}^k(D)} \lesssim h_D^{(m+1)-k} |\mathbf{u}|_{\mathbf{H}^{m+1}(D)},$$

where $h_D = diam(D)$ is the diameter of domain D.

 (ii) *Moreover, if $\mathbf{v} \in \mathbf{S}^{m+1}(D)$, then there exists $\mathbf{q} \in \mathbf{Q}^m(D)$ such that for any integer $0 \leq k \leq m+1$,*

$$(9) \qquad \|\mathbf{v} - \mathbf{q}\|_{\mathbf{H}^k(D)} \lesssim h_D^{(m+1)-k} |\mathbf{v}|_{\mathbf{H}^{m+1}(D)}.$$

Proof: A proof based on a density argument and the Taylor expansion can be found in [1]. It is not surprising to see that the proof requires D has a subset of positive measure, with respect to which domain D is star-shaped. The proof also utilizes the fact that the Taylor polynomial of a divergence-free vector field is divergence-free. $\square$

Theorem 2 (Inverse estimates)   *Let D be a bounded domain with a Lipschitz boundary. For any $\mathbf{q} \in \mathbf{Q}^m(D)$ and integers $0 \leq k < l$, we have the following inverse estimates*

$$(10) \qquad \|\mathbf{q}\|_{\mathbf{H}^l(D)} \lesssim h_D^{k-l} \|\mathbf{q}\|_{\mathbf{H}^k(D)},$$

especially

$$(11) \qquad \|\mathbf{q}\|_{\mathbf{H}^1(D)} \lesssim h_D^{-1} \|\mathbf{q}\|_{\mathbf{L}_2(D)},$$

and

$$(12) \qquad \|\mathbf{q}\|_{\mathbf{L}_2(\partial D)} \lesssim h_D^{-1/2} \|\mathbf{q}\|_{\mathbf{L}_2(D)}.$$

Proof: The first inequality can be derived from the standard componentwise inverse estimates [6]. For the third inequality, we apply the trace theorem to $\mathbf{q}$ and the second inequality:

$$\|\mathbf{q}\|_{\mathbf{L}_2(\partial D)} \lesssim \|\mathbf{q}\|_{\mathbf{L}_2(D)}^{\frac{1}{2}}\|\mathbf{q}\|_{\mathbf{H}^1(D)}^{\frac{1}{2}} \lesssim h_D^{-\frac{1}{2}}\|\mathbf{q}\|_{\mathbf{L}_2(D)}.$$

$\square$

Remark   The two inequalities in Theorem 1 are of Jackson type, while the inequalities in Theorem 2 are of Bernstein type [9]. These two (direct and inverse) types of estimates are frequently seen and essentially needed for most approximation problems.

Let $\mathcal{E}_h$ be a quasi-uniform partition of Ω with mesh size h and Γ_h be the set of all interior interfaces. We define

(13)
$$\mathbf{V}_h^m(\Omega) = \{\mathbf{w} : \mathbf{w}|_E \in \mathbf{Q}^m(E), \ \forall E \in \mathcal{E}_h\}.$$
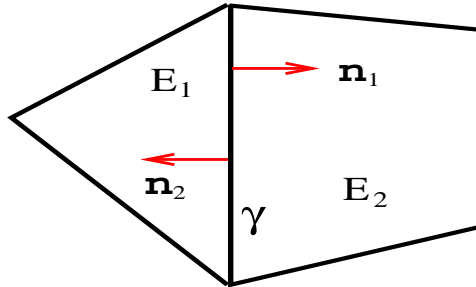

FIGURE 1. An edge shared by two elements

Piecewise vector fields: jumps and total divergence   Let $\mathbf{u}$ be a piecewise vector field defined on $\mathcal{E}_h$ that might be discontinuous across the internal element interfaces. Let E_1 and E_2 be two elements sharing edge/face γ. The jump of the vector field $\mathbf{u}$ on γ at point P is defined as

(14)
$$[\mathbf{u}]_\gamma(P) = \mathbf{u}|_{E_1}(P) \cdot \mathbf{n}_1 + \mathbf{u}|_{E_2}(P) \cdot \mathbf{n}_2,$$

where $\mathbf{n}_1$ and $\mathbf{n}_2$ are the unit outward normal vectors. The maximal and total jumps of $\mathbf{u}$ over Γ_h are respectively defined as

(15)
$$\max_{\gamma \in \Gamma_h} \max_{P \in \gamma} |[\mathbf{u}]_\gamma(P)|, \qquad \sum_{\gamma \in \Gamma_h} \int_\gamma |[\mathbf{u}]_\gamma| \, d\gamma.$$

In addition, we adopt the definition of total divergence in [8] for a piecewise vector field $\mathbf{u}$:

(16)
$$\sum_{\gamma \in \Gamma_h} \int_\gamma |[\mathbf{u}]_\gamma| d\gamma + \sum_{E \in \mathcal{E}_h} \int_E |\nabla \cdot \mathbf{u}| dE.$$

When a piecewise vector field is locally divergence-free inside each element, the total jump is the same as the total divergence.

Localized $\mathbf{L}_2$-Projection   We shall also need the localized $\mathbf{L}_2$-projection Π_h from $\mathbf{S}^{m+1}(\Omega)$ to $\mathbf{V}_h^m(\Omega)$ ($m \geq 0$) that was introduced in [3]. Let $\mathbf{v} \in \mathbf{S}^{m+1}(\Omega)$ and $E \in \mathcal{E}_h$. First $\pi_E \mathbf{v} \in \mathbf{Q}^m(E)$ is defined by

(17)
$$(\pi_E \mathbf{v}, \mathbf{q}) = (\mathbf{v}, \mathbf{q}), \quad \forall \mathbf{q} \in \mathbf{Q}^m(E).$$

Then $\Pi_h \mathbf{v} \in \mathbf{V}_h^m(\Omega)$ is defined by

$$(18) \qquad\qquad \Pi_h = \sum_{E \in \mathcal{E}_h} \pi_E \mathbf{1}_E,$$

where $\mathbf{1}_E$ is the indicator function of element E.

Theorem 3   *Let $\mathcal{E}_h$ be a quasi-uniform partition of Ω and E be any element in $\mathcal{E}_h$. Let Π_h be the localized $\mathbf{L}_2$-projection defined above and $m \geq 0$ an integer. If $\mathbf{v} \in \mathbf{S}^{m+1}(\Omega)$, then*

 (i) *For any $\mathbf{q} \in \mathbf{Q}^m(E)$, $\pi_E \mathbf{q} = \mathbf{q}$,*
 (ii) $\|\pi_E \mathbf{v}\|_{\mathbf{L}_2(E)} \leq \|\mathbf{v}\|_{\mathbf{L}_2(E)}$,
 (iii) $\|\mathbf{v} - \pi_E \mathbf{v}\|_{\mathbf{L}^2(E)} \lesssim h^{m+1} |\mathbf{v}|_{\mathbf{H}^{m+1}(E)}$,
 (iv) $\|\mathbf{v} - \Pi_h \mathbf{v}\|_{\mathbf{L}^2(\Omega)} \lesssim h^{m+1} |\mathbf{v}|_{\mathbf{H}^{m+1}(\Omega)}$.

 Proof: (i) and (ii) are straightforward and will be used in the proof of (iii).

To prove (iii), we apply Theorem 1(ii). There exists a solenoidal polynomial vector field $\mathbf{q}_E$ of degree m such that

$$\|\mathbf{v} - \mathbf{q}_E\|_{\mathbf{L}_2(E)} \lesssim h^{m+1} |\mathbf{v}|_{\mathbf{H}^{m+1}(E)}.$$

From (i), we have

$$\mathbf{v} - \pi_E \mathbf{v} = \mathbf{v} - \mathbf{q}_E + \pi_E \mathbf{q}_E - \pi_E \mathbf{v}.$$

Applying (ii) and Theorem 1(ii) to element E, we obtain

$$\|\mathbf{v} - \pi_E \mathbf{v}\|_{\mathbf{L}_2(E)} \leq \|\mathbf{v} - \mathbf{q}_E\|_{\mathbf{L}_2(E)} + \|\pi_E(\mathbf{v} - \mathbf{q}_E)\|_{\mathbf{L}_2(E)}$$

$$\lesssim \|\mathbf{v} - \mathbf{q}_E\|_{\mathbf{L}_2(E)} \lesssim h^{m+1} |\mathbf{v}|_{\mathbf{H}^{m+1}(E)}.$$

Summing the above estimate over all elements, we have

$$\|\mathbf{v} - \Pi_h \mathbf{v}\|_{\mathbf{L}^2(\Omega)}^2 = \sum_{E \in \mathcal{E}_h} \|\mathbf{v} - \pi_E \mathbf{v}\|_{\mathbf{L}_2(E)}^2$$

$$\lesssim \sum_{E \in \mathcal{E}_h} (h^{m+1})^2 |\mathbf{v}|_{\mathbf{H}^{m+1}(E)}^2 = h^{2(m+1)} |\mathbf{v}|_{\mathbf{H}^{m+1}(\Omega)}^2,$$

which completes the proof of (iv).   □

Corollary 1   *Let $\mathbf{v} \in \mathbf{S}^{m+1}(\Omega)$ and $E \in \mathcal{E}_h$. For any real number s in the range $0 \leq s \leq m+1$, we have*

$$(19) \qquad\qquad \|\mathbf{v} - \pi_E \mathbf{v}\|_{\mathbf{H}^s(E)} \lesssim h^{(m+1)-s} |\mathbf{v}|_{\mathbf{H}^{m+1}(E)}.$$

 Proof: We first prove the claim for any nonnegative integer $0 \leq k \leq m+1$. This is similar to the proof of Theorem 3(iii). From Theorem 1(ii), there exists a solenoidal polynomial vector field $\mathbf{q}_E$ of degree m such that

$$\|\mathbf{v} - \mathbf{q}_E\|_{\mathbf{H}^k(E)} \lesssim h^{(m+1)-k} |\mathbf{v}|_{\mathbf{H}^{m+1}(E)}.$$

Again we have

$$\mathbf{v} - \pi_E \mathbf{v} = (\mathbf{v} - \mathbf{q}_E) + (\mathbf{q}_E - \pi_E \mathbf{v}),$$

and we only need to estimate the $\mathbf{H}^k(E)$-norm of the second term. Applying the inverse estimate to $(\mathbf{q}_E - \pi_E \mathbf{v})$, we obtain

$$\|\mathbf{q}_E - \pi_E \mathbf{v}\|_{\mathbf{H}^k(E)} \lesssim h^{-k} \|\mathbf{q}_E - \pi_E \mathbf{v}\|_{\mathbf{L}_2(E)}$$

$$= h^{-k} \|\pi_E \mathbf{q}_E - \pi_E \mathbf{v}\|_{\mathbf{L}_2(E)} \leq h^{-k} \|\mathbf{q}_E - \mathbf{v}\|_{\mathbf{L}_2(E)}$$

$$\lesssim h^{(m+1)-k} |\mathbf{v}|_{\mathbf{H}^{m+1}(E)}.$$

Applying the operator interpolation theory [2], we extend this result to any real exponent $s \in (0, m + 1)$. □

Similar discussions can be found in [3], but we have further estimates about jumps on element interfaces stated in Theorem 4. To prove Theorem 4, we need Lemma 1(i).

Lemma 1   *Let* $\mathbf{v} \in \mathbf{S}^{m+1}(\Omega)$ *and* $E \in \mathcal{E}_h$. *Then the following holds*

(i) $\|\mathbf{v} - \pi_E \mathbf{v}\|_{\mathbf{L}_1(\partial E)} \lesssim h^{m + \frac{d}{2}} |\mathbf{v}|_{\mathbf{H}^{m+1}(E)}$,

(ii) $\|\mathbf{v} - \pi_E \mathbf{v}\|_{\mathbf{L}_2(\partial E)} \lesssim h^{m + \frac{1}{2}} |\mathbf{v}|_{\mathbf{H}^{m+1}(E)}$,

where $d = 2$ *or* 3 *is the space dimension.*

Proof: One can derive (i) from (ii), the Cauchy-Schwarz inequality, and the fact (based on the quasi-uniformity of $\mathcal{E}_h$) that

$$\int_{\partial E} 1 = \mathcal{O}(h^{d-1}),$$

for $d = 2$ or 3. So we only need to prove (ii). From Corollary 1, we have

$$\|\mathbf{v} - \pi_E \mathbf{v}\|_{\mathbf{L}_2(E)} \lesssim h^{m+1} |\mathbf{v}|_{\mathbf{H}^{m+1}(E)}, \qquad \|\mathbf{v} - \pi_E \mathbf{v}\|_{\mathbf{H}^1(E)} \lesssim h^m |\mathbf{v}|_{\mathbf{H}^{m+1}(E)}.$$

Applying the trace theorem [6] to $(\mathbf{v} - \pi_E \mathbf{v})$ and the above two estimates, we obtain

$$\|\mathbf{v} - \pi_E \mathbf{v}\|_{\mathbf{L}_2(\partial E)} \lesssim \|\mathbf{v} - \pi_E \mathbf{v}\|_{\mathbf{L}_2(E)}^{\frac{1}{2}} \|\mathbf{v} - \pi_E \mathbf{v}\|_{\mathbf{H}^1(E)}^{\frac{1}{2}}$$

$$\lesssim (h^{m+1})^{\frac{1}{2}} |\mathbf{v}|_{\mathbf{H}^{m+1}(E)}^{\frac{1}{2}} (h^m)^{\frac{1}{2}} |\mathbf{v}|_{\mathbf{H}^{m+1}(E)}^{\frac{1}{2}}$$

$$= h^{m + \frac{1}{2}} |\mathbf{v}|_{\mathbf{H}^{m+1}(E)}.$$

□

Theorem 4 (The total divergence of the localized $\mathbf{L}_2$-projection) *Let* $\mathcal{E}_h$, Γ_h, *and* Π_h *be defined as above. For any* $\mathbf{v} \in \mathbf{S}^{m+1}(\Omega)$, *the following estimate regarding the total divergence or the total jump of* $\Pi_h \mathbf{v}$ *over* Γ_h *holds:*

(20) $$\sum_{\gamma \in \Gamma_h} \int_{\gamma} |[\Pi_h \mathbf{v}]_{\gamma}| d\gamma \lesssim h^m |\mathbf{v}|_{\mathbf{H}^{m+1}(\Omega)}.$$

Proof: Let γ be an edge (for $d = 2$) or a face (for $d = 3$) shared by two elements E_1 and E_2, as shown in Figure 1. On γ, we have $\mathbf{v} \cdot \mathbf{n}_1 + \mathbf{v} \cdot \mathbf{n}_2 = 0$. From (14), we have

$$[\Pi_h \mathbf{v}]_{\gamma} = \pi_{E_1} \mathbf{v} \cdot \mathbf{n}_1 + \pi_{E_2} \mathbf{v} \cdot \mathbf{n}_2$$

$$= (\pi_{E_1} \mathbf{v} - \mathbf{v}) \cdot \mathbf{n}_1 + (\pi_{E_2} \mathbf{v} - \mathbf{v}) \cdot \mathbf{n}_2.$$

By the Cauchy-Schwarz inequality, we have

$$|[\Pi_h \mathbf{v}]_{\gamma}| \leq |(\pi_{E_1} \mathbf{v} - \mathbf{v}) \cdot \mathbf{n}_1| + |(\pi_{E_2} \mathbf{v} - \mathbf{v}) \cdot \mathbf{n}_2|$$

$$\leq |\pi_{E_1} \mathbf{v} - \mathbf{v}| + |\pi_{E_2} \mathbf{v} - \mathbf{v}|,$$

and hence

$$\int_{\gamma} |[\Pi_h \mathbf{v}]_{\gamma}| d\gamma \leq \int_{\gamma} |\mathbf{v} - \pi_{E_1} \mathbf{v}| d\gamma + \int_{\gamma} |\mathbf{v} - \pi_{E_2} \mathbf{v}| d\gamma.$$

Summing over all edges/faces and applying Lemma 1(i) and the Cauchy-Schwarz inequality again, we obtain

$$\sum_{\gamma \in \Gamma_h} \int_\gamma |[\Pi_h \mathbf{v}]_\gamma| d\gamma \lesssim \sum_{E \in \mathcal{E}_h} \|\mathbf{v} - \pi_E \mathbf{v}\|_{\mathbf{L}_1(\partial E)}$$

$$\lesssim h^{m+\frac{d}{2}} \sum_{E \in \mathcal{E}_h} |\mathbf{v}|_{\mathbf{H}^{m+1}(E)} \leq h^{m+\frac{d}{2}} \left(\sum_{E \in \mathcal{E}_h} |\mathbf{v}|^2_{\mathbf{H}^{m+1}(E)} \right)^{\frac{1}{2}} \left(\sum_{E \in \mathcal{E}_h} 1 \right)^{\frac{1}{2}}$$

$$= h^{m+\frac{d}{2}} |\mathbf{v}|_{\mathbf{H}^{m+1}(\Omega)} \left(\sum_{E \in \mathcal{E}_h} 1 \right)^{\frac{1}{2}}.$$

The quasi-uniformity of the partition $\mathcal{E}_h$ implies that $\sum_{E \in \mathcal{E}_h} 1$, i.e., the number of elements in $\mathcal{E}_h$ is $\mathcal{O}(h^{-d})$, which yields the desired result in the theorem.   □
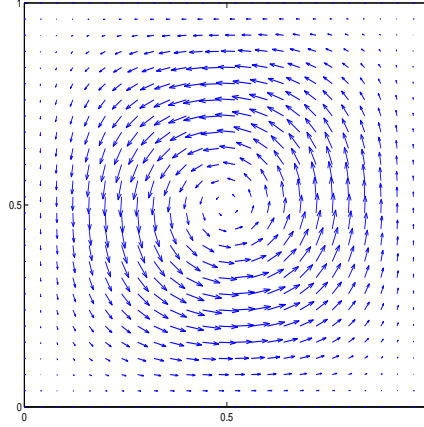

FIGURE 2. The swirling velocity field in Example 1

4. Numerical Results

In this section, we present some numerical results to illustrate and validate the theoretical error estimates proved in the last section. The normalized basis functions discussed in Section 2 are used to carry out these numerical experiments. The four quasi-uniform triangular meshes in both examples are produced using the PDE toolbox in Matlab.

Example 1: the swirling vector field   This example can be found in [12]. The domain Ω is the unit square $[0,1] \times [0,1]$ and the velocity field $\mathbf{v}(x,y) = (v_1, v_2)$ is given by

$$v_1(x,y) = \sin^2(\pi x) \sin(2\pi y), \quad v_2(x,y) = -\sin(2\pi x) \sin^2(\pi y).$$

This incompressible (div $\mathbf{v} = 0$) velocity field vanishes ($\mathbf{v} = \mathbf{0}$) on the four sides and at the center of the square, see Figure 2. Notice that this vector field is actually infinitely smooth, so $\mathbf{v} \in \mathbf{S}^{m+1}(\Omega)$ for any integer $m \geq 0$. Therefore, approximation accuracy is actually determined by the degree of polynomials we use in the LDF elements. This fact is clearly reflected by the numerical results in Tables 2-5.

Example 2: a nonsmooth vector field   The domain Ω is also the unit square and the nonsmooth velocity field is given by $\mathbf{v}(x,y) = (|y - 0.5|, |x - 0.5|)$,

TABLE 1. Example 1 and 2: statistics of the meshes on the unit square

Triangular meshes	#elements	#edges	mesh size	Rectangular meshes	#elements	#edges
TrigMesh1	328	512	$h \approx 0.11$			
TrigMesh2	1312	2008	$h/2$	RectMesh2	50x50	2x50x51
TrigMesh3	5248	7952	$h/4$	RectMesh3	100x100	2x100x101
TrigMesg4	20992	31648	$h/8$	RectMesh4	200x200	2x200x201

TABLE 2. Example 1: the localized $\mathbf{L}_2$-projection of the swirling field on triangular meshes

Approx. error	deg. 1		deg. 2		deg. 3	
	$\mathbf{L}_\infty$	$\mathbf{L}_2$	$\mathbf{L}_\infty$	$\mathbf{L}_2$	$\mathbf{L}_\infty$	$\mathbf{L}_2$
TrigMesh2	6.895E-3	1.527E-3	1.692E-4	4.406E-5	2.442E-6	5.592E-7
TrigMesh3	1.742E-3	3.821E-4	2.130E-5	5.514E-6	1.537E-7	3.496E-8
TrigMesh4	4.367E-4	9.557E-5	2.670E-6	6.895E-7	9.626E-9	2.185E-9
Error order	2	2	3	3	4	4

TABLE 3. Example 1: the localized $\mathbf{L}_2$-projection of the swirling field on rectangular meshes

Approx. error	deg. 1		deg. 2		deg. 3	
	$\mathbf{L}_\infty$	$\mathbf{L}_2$	$\mathbf{L}_\infty$	$\mathbf{L}_2$	$\mathbf{L}_\infty$	$\mathbf{L}_2$
RectMesh2	2.320E-3	6.238E-4	5.043E-5	1.154E-5	7.219E-7	1.727E-7
RectMesh3	5.809E-4	1.560E-4	6.309E-6	1.443E-6	4.550E-8	1.080E-8
RectMesh4	1.452E-4	3.901E-5	7.887E-7	1.805E-7	3.191E-9	6.826E-10
Error order	2	2	3	3	4	4

TABLE 4. Example 1: jumps of the localized $\mathbf{L}_2$-projection on triangular meshes

Jumps	deg. 1		deg. 2		deg. 3	
	max	total	max	total	max	total
TrigMesh2	7.330E-3	8.830E-2	3.864E-4	2.658E-3	8.879E-6	4.493E-5
TrigMesh3	1.945E-3	4.520E-2	4.816E-5	6.772E-4	5.726E-7	5.654E-6
TrigMesh4	4.915E-4	2.286E-2	6.032E-6	1.707E-4	3.622E-8	7.093E-7
Error order	2	1	3	2	4	3

TABLE 5. Example 1: jumps of the localized $\mathbf{L}_2$-projection on rectangular meshes

Jumps	deg. 1		deg. 2		deg. 3	
	max	total	max	total	max	total
RectMesh2	3.664E-3	8.140E-2	8.273E-5	1.341E-3	1.526E-6	1.777E-5
RectMesh3	9.197E-4	4.077E-2	1.037E-5	3.357E-4	9.582E-8	2.221E-6
RectMesh4	2.300E-4	2.039E-2	1.297E-6	8.394E-5	6.223E-9	2.838E-7
Error order	2	1	3	2	4	3

which is divergence-free. It can be proved that for any $0 < \epsilon < 1$, $\mathbf{v} \in \mathbf{H}^{\frac{3}{2}-\epsilon}(\Omega)$. It is also clear that $\mathbf{v} \in \mathbf{W}_\infty^1(\Omega)$, but $\mathbf{v} \notin \mathbf{W}_\infty^m(\Omega)$ for any integer $m > 1$. The low order regularity of the vector field limits the approximation accuracy of the localized $\mathbf{L}_2$-projection, even though higher order LDF elements are used. It can

be observed from Table 6 that for the errors in $\mathbf{L}_\infty$-norm, the convergence rate can only be the first order, since $\mathbf{v}$ is only in $\mathbf{W}_\infty^1(\Omega)$. Increasing the polynomial degree of the LDF elements does reduce the approximation errors, but it does not increase the convergence order. For the errors in $\mathbf{L}_2$-norm, since $\mathbf{v}$ is almost in $\mathbf{H}^{\frac{3}{2}}$, one can get a 1.5 order convergence rate if the LDF elements have degree 1 or higher, but only the first order convergence if degree 0 LDF elements are used. All these conform with the general fact that the convergence rate is $\min(\alpha, m+1)$, where α is the smoothness order of the function being approximated and m is the degree of the polynomials being used for approximation.

TABLE 6. Example 2: the localized $\mathbf{L}_2$-projection of the non-smooth field on triangular meshes

	deg. 0		deg. 1		deg. 2	
Approx. error	$\mathbf{L}_\infty$	$\mathbf{L}_2$	$\mathbf{L}_\infty$	$\mathbf{L}_2$	$\mathbf{L}_\infty$	$\mathbf{L}_2$
TrigMesh1	5.368E-2	2.522E-2	2.825E-2	2.757E-3	7.833E-3	9.421E-4
TrigMesh2	2.684E-2	1.272E-2	1.556E-2	9.500E-4	4.865E-3	3.917E-4
TrigMesh3	1.342E-2	6.388E-3	7.833E-3	3.339E-4	2.573E-3	1.371E-4
TrigMesh4	6.710E-3	3.200E-3	3.804E-3	1.198E-4	1.255E-3	5.036E-5
Error order	1	1	≈ 1	≈ 1.5	≈ 1	≈ 1.5

TABLE 7. Example 2: jumps of the localized $\mathbf{L}_2$-projection on triangular meshes

	deg. 0		deg. 1		deg. 2	
Jumps	max	total	max	total	max	total
TrigMesh2	2.949E-2	7.367E-1	1.313E-2	1.185E-2	7.243E-3	4.467E-3
TrigMesh3	1.474E-2	7.729E-1	8.028E-3	6.029E-3	3.768E-3	2.467E-3
TrigMesh4	7.372E-3	7.907E-1	4.012E-3	3.421E-3	1.782E-3	1.286E-3
Error order	1	0	≈ 1	≈ 1	≈ 1	≈ 1

5. Concluding Remarks

In this paper, we present a complete account of the approximation properties of the locally divergence-free finite elements. Both direct and inverse estimates (Jackson- and Bernstein- type inequalities) are discussed. We have also established and validated (through numerical experiments) the error estimates about the jumps and the total divergence of the localized $\mathbf{L}_2$-projection, which can be used for approximations to initial solenoidal vector fields in time-dependent problems. Normalized bases for the LDF finite elements that have better numerical stability are proposed and used in our numerical experiments.

Acknowledgments

References

[1] G.A. Baker, W.N. Jureidini, and O.A. Karakashian, *Piecewsie solenoidal vector fields and the Stokes problem*, SIAM Numer. Anal., **27**(1990), pp. 1466–1485.

[2] C. Bennett and R. Sharpley, *Interpolation of operators*, Academic Press, 1988.

[3] N. Besse and D. Kröner, *Convergence of locally divergence-free discontinuous-Galerkin methods for the induction equations of the 2D-MHD system*, M2AN Math. Model. Numer. Anal., **39**(2005), pp. 1177–1202.

[4] J.U. Brackbill and D.C. Barnes, *The effect of nonzero $\nabla \cdot \mathbf{B}$ on the numerical solution of the magnetohydrodynamic equations*, J. Comput. Phys., **35**(1980), pp. 426–430.

[5] S.C. Brenner, F. Li and L.-Y. Sung, *A locally divergence-free nonconforming finite element method for the reduced time-harmonic Maxwell equations*, Math. Comp. **76**(2007), pp. 573–595.

[6] S.C. Brenner and L.R. Scott, *Mathematical theory of finite element methods*, Springer, Berlin, 2002.

[7] B. Cockburn, G. Kanschat, and D. Schötzau, *A locally conservative LDG method for the incompressible Navier-Stokes equations*, Math. Comp., **74**(2005), pp. 1067-1095.

[8] B. Cockburn, F. Li, and C.W. Shu, *Locally divergence-free discontinuous Galerkin methods for the Maxwell equations*, J. Comput. Phys., **194**(2004), pp. 588–610.

[9] R.A. DeVore, *Nonlinear approximation*, Acta Numer., **7**(1998), pp. 51–150.

[10] O.A. Karakashian and W.N. Jureidini, *A nonconforming finite element method for the stationary Navier-Stokes equations*, SIAM Numer. Anal., **35**(1998), pp. 93–120.

[11] O. Karakashian and Th. Katsaounis, *Numerical simulation of incompressible fluid flow using locally solenoidal elements*, Comput. Math. Appl., **51**(2006), pp. 1551–1570.

[12] R.J. LeVeque, *High-resolution conservative algorithms for advection in incompressible flow*, SIAM J. Numer. Anal., **33**(1996), pp. 627–665.

[13] F. Li and C.W. Shu, *Locally divergence-free discontinuous Galerkin methods for MHD equations*, J. Sci. Comput., **22/23**(2005), pp. 413–442.

[14] J. Liu, S. Sun, and S. Tavener, *A discontinuous Galerkin-Lagrangian method for the resistive magnetic induction equation and its convergence analysis*, Preprint, Colorado State University, 2007.

Department of Mathematics, Colorado State University, Fort Collins, CO 80523-1874, USA
E-mail: `liu@math.colostate.edu`
URL: `http://www.math.colostate.edu/∼liu/`